

Article

Simple Aseismic Reinforcement of Steel Structures Using Knee Braces with High-Hardness Vises

Hiroyuki Nakahara *, Ding Nan and Iathong Chan 

Graduate School of Engineering, Nagasaki University, Nagasaki 852-8521, Japan;
bb52222101@ms.nagasaki-u.ac.jp (D.N.); chan.iathong@nagasaki-u.ac.jp (I.C.)

* Correspondence: nakaharahiroyuki@nagasaki-u.ac.jp; Tel.: +81-819-2895

Abstract: A novel technique for upgrading the seismic resistance of steel buildings by adding knee braces to existing structures using vises was proposed by researchers in 2022. A feature of this retrofitting method is the easy setup owing to its use of vises made from high-hardness metal. Tests were conducted to investigate two main failure modes: slipping failure at the connection and yielding and buckling failure of the knee brace. The retrofitting design is discussed based on a comparison between the slipping strengths obtained through tests and calculations. Furthermore, an analytical study, using the finite element method (FEM), was conducted to evaluate the test results of retrofitted frames that failed in terms of the yielding and buckling of the knee braces. The findings of the analyses are consistent with the test results. This study included a stress relaxation test to assess the long-term performance of the vises.

Keywords: seismic retrofit; FEM analysis; yielding strength; buckling strength; long-term performance



Citation: Nakahara, H.; Nan, D.; Chan, I. Simple Aseismic Reinforcement of Steel Structures Using Knee Braces with High-Hardness Vises. *Buildings* **2024**, *14*, 3029. <https://doi.org/10.3390/buildings14093029>

Academic Editors: Wusheng Zhao, Linfeng Lu and Shaofeng Nie

Received: 4 July 2024

Revised: 26 July 2024

Accepted: 10 September 2024

Published: 23 September 2024



Copyright: © 2024 by the authors. Licensee MDPI, Basel, Switzerland. This article is an open access article distributed under the terms and conditions of the Creative Commons Attribution (CC BY) license (<https://creativecommons.org/licenses/by/4.0/>).

1. Introduction

In Japan, many buildings have been damaged by large-scale earthquakes. In one steel building, the beam–column connection was broken, as shown in Figure 1 [1]. This fracture caused critical damage not only to the structure but also to human lives. The number of fractures observed in old buildings with defects in welding is decreasing. Seismic retrofitting in existing buildings is an effective method to reduce the damage caused by earthquakes. Many important studies have been conducted on seismic retrofits by researchers worldwide. For example, Fang [2] submitted a report on the practical applications of seismic retrofitting in the past decade, while MacRae [3] detailed diverse brace structures. The energy dissipation capacities of steel dampers were explored in studies by Domenico et al. [4], Kishiki et al. [5], and Tamai et al. [6] by investigating plastic deformation behaviors.

The authors of this study suggest a new technique for improving the seismic stability of steel structures by employing knee braces that are connected to existing structures through vises, which are composed of a body and a screw bolt made of high-strength metal. This method is specifically designed for moment-resisting frames in steel buildings.

Figure 2 illustrates a bending moment diagram for a portal frame subjected to a horizontal force. In a simple frame, the maximum bending moments are typically observed at the ends of both the beam and column. Defects and imperfections in welding joints between beams and columns have been found to result from damage caused by earthquakes. Knee braces are added to the frame, as shown in Figure 3, which decrease the bending moments at the beam–column connections. Knee-braced moment-resisting frames were studied in previous research [7–14], which reported that the structural stiffness and energy dissipation of these frames were enhanced compared those of normal moment-resisting frames with equivalent structural members. Previous studies conducted by Harada [15] and Yamada [16] investigated seismic retrofitting methods that use knee braces. Harada's

research focused on bolted joints between retrofitted frames and knee braces, whereas Yamada et al. studied the use of knee brace dampers for retrofitting over-track buildings.



Figure 1. Steel structure damaged by Kobe earthquake in 1995 (reprinted from Ref. [1]).

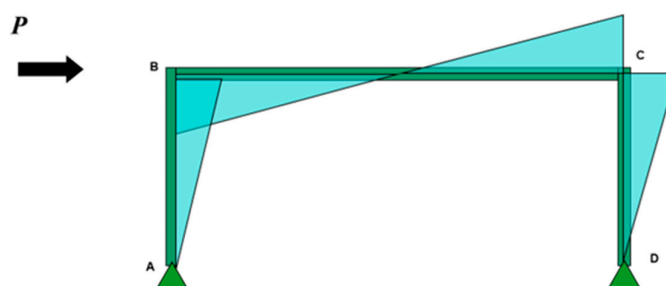


Figure 2. Bending moment diagram of non-retrofitted steel structure.

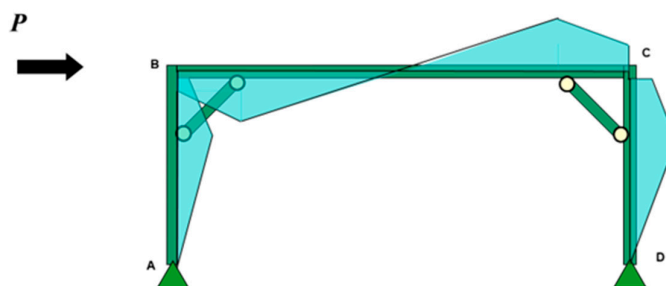


Figure 3. Bending moment diagram of retrofitted steel structure.

Knee braces serve the dual purpose of decreasing bending moments at the ends of structural members and enhancing the rigidity of beam–column connections. They are effective in preventing damage to the beam–column connections, but their implementation in existing buildings is challenging. The authors of this study suggest using the vise shown in Figure 4 as a potential solution.

The vise is designed to clamp the endplates of the knee brace onto existing beams and columns without requiring any welding or drilling for bolts. The bolthead of the vise is made from high-hardness metal. The loosening of the bolt is prevented because the head of the bolt bites into the steel plate when an initial torque is introduced.

Tests were conducted to investigate two main failure modes: slipping failure at the connection and yielding and buckling failure of the knee brace. The former was the test for the connecting design by the vises. The latter was conducted to estimate the energy

dissipation performance of the knee braces. A simple equation for the slipping failure was proposed based on the test results reported in our previous paper [17]. The failure at the connections is normally avoided in seismic design. When the slipping strength is designed to be safe for the failure of the connections, the knee brace exhibits yield failure under tensile force and buckling failure under compressive force. The load versus deformation relations of the knee braces were obtained from the tests. A nonlinear finite element method (FEM) analysis was performed to assess the yielding and buckling behaviors of the knee brace. The analytical results obtained through FEM were compared with the experimental results reported in this paper. The FEM analysis was also conducted to examine the stress states of the vise itself, as reported in Appendix A. Furthermore, the long-term performance of high-hardness vises was examined through relaxation tests, which were then compared to the relaxation tests of high-strength bolts mentioned in previous studies.



Figure 4. Vise used for the seismic retrofitting of steel structures.

In Section 2, the experimental studies of the retrofitted frame using knee braces are shown. In Section 3, an FEM analysis is conducted and the findings are compared with the experimental results. In Section 4, the results of the relaxation tests are presented. Section 5 summarizes the outcomes of the study.

2. Experimental Study of Retrofitted Frame Using Knee Braces

A study on the use of knee braces to retrofit partial frames was conducted and is described in Ref. [17]. Figure 5 shows the test setup. Figure 6 shows the knee braces used as specimens for the investigation of slipping failure at the connection, and Figure 7 shows the knee braces used for the investigation of yielding and buckling. The length L , thickness t , and height h of the specimens are listed in Table 1. Table 2 shows the material properties of the beam and column used in the tests, and Table 3 shows the material properties of the knee braces used in the tests. The notations in the tables are as follows: tf : thickness of the flange of the H-shaped steel; t : thickness of the steel plate; σ_y : yield strength; σ_u : tensile strength; est : strain at the point of strain hardening.

Table 1. Dimensions of knee braces in retrofitted steel frame specimens.

	h (mm)	L (mm)	t (mm)	θ (°)
SL-45-1	50.3	450	21.8	45
SL-45-2	50.3	450	21.8	45
SL-45-3	50.3	450	21.8	45
SL-30	50.0	384	21.5	30
nSL-6	5.9	200	21.5	45
nSL-9	9.0	200	21.5	45
nSL-12	11.9	200	21.5	45
nSL-15	14.8	200	21.5	45

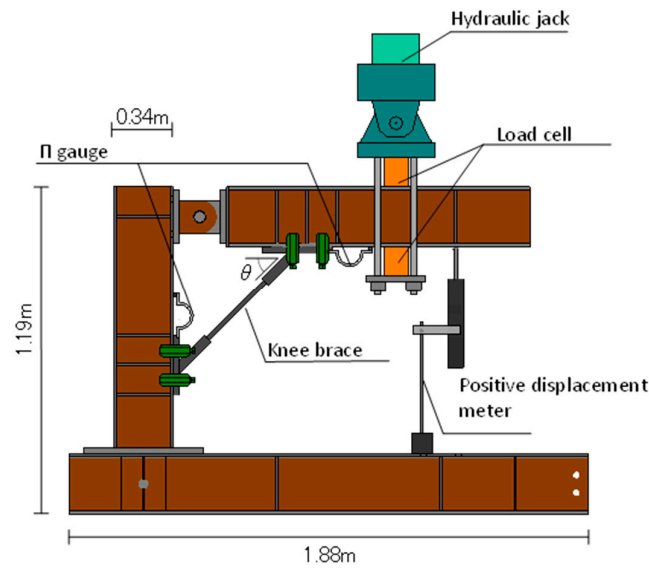


Figure 5. Test setup with loading and measuring devices (reprinted from Ref. [17]).

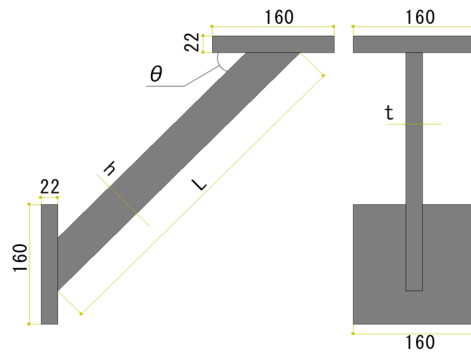


Figure 6. Shape of knee brace for investigating slipping failure at connection (unit: mm).

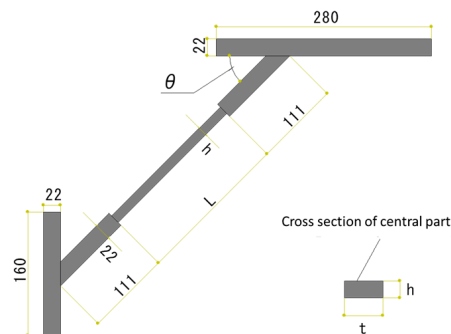


Figure 7. Shape of knee brace for investigating yielding at knee brace (unit: mm).

Table 2. Material properties of steel frame in test.

		t_f (mm)	σ_y (N/mm ²)	σ_u (N/mm ²)	ϵ_{st} (%)
H-shaped Beam	SM490	8.9	392	520	2.83
H-shaped Column	H-SA700	9.0	795	862	—

Table 3. Material properties of steel plates for knee braces.

		t (mm)	σ_y (N/mm ²)	σ_u (N/mm ²)	ϵ_{st} (%)
SL-45	SM400	21.8	279	428	1.89
SL-30	SM400	21.5	271	434	1.85
nSL					

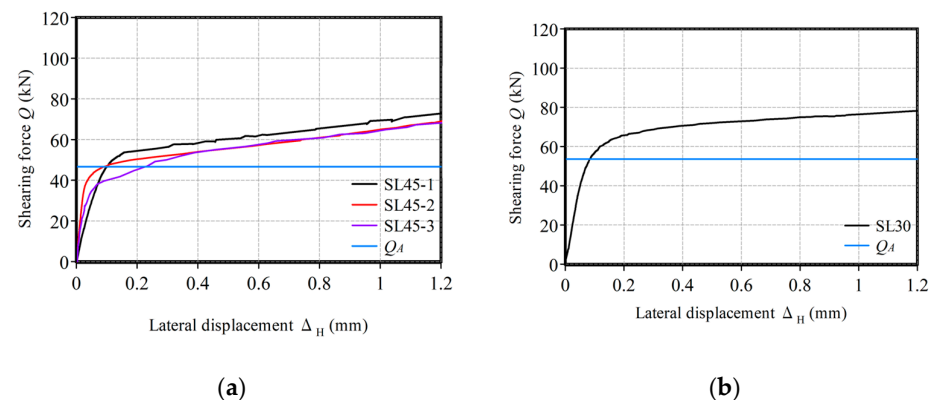
The initial torque introduced using a torque wrench was 300 Nm for all vise bolts. The parameter for studying slipping behavior is the angle θ between the beams and knee braces. The angles of the specimens were 45° and 30°, respectively. The shapes of the specimens SL-45-1, SL-45-2, and SL-45-3 were the same. The slipping strength test results were validated against the evaluation method for the slipping strength, which was determined using Equation (1).

$$Q_A = \frac{nB\mu}{1 + \mu \tan \theta}, \quad (1)$$

Equation (1) was derived in our previous paper [17], where n is the number of vises, B is the axial force of the bolt of the vise, μ is the frictional coefficient, and θ is the angle between the knee brace and the horizontal beam. When the values are $n = 2$, $B = 75$ kN, $\mu = 0.45$, $\theta = \pi/4$, and $\tan \theta = 1$, then $Q_A = 46.6$ kN. When $\theta = \pi/6$, $Q_A = 53.6$ kN.

The load cells are set vertically along the axis of the hydraulic jack to measure the applied force, as shown in Figure 5. The slipping displacement is measured by π gauges laterally at the surface between the endplate of the knee brace and the steel beam. The strains on the surface of the knee brace along its axis are measured by four strain gauges glued to them. Axial deformations of the knee brace are measured using two displacement meters. The axial force N of the knee brace is obtained by multiplying the strain by its axial stiffness when the knee brace remains elastic. N can be determined in a rotational equilibrium state.

The experimental results for (a) SL-45-1, SL-45-2, SL-45-3, and (b) SL-30 are shown in Figure 8. The vertical axis shows the lateral component Q of N , and the horizontal axis shows the lateral displacement Δ_H , which is the average of the two displacements measured by the π gauges. The value of N is obtained from the strain gauge data shown in the figure. The slipping strengths are summarized in Table 4. The slipping strengths of the tests are defined as the forces at a slipping deformation of 0.5 mm, in accordance with AISC [18], and they exceed the slipping strengths, Q_A , calculated using Equation (1). The average strength of SL-45-1, SL-45-2, and SL-45-3 is 56.3 kN. The calculated value is 46.6 kN. The coefficient of variation is 4.5%. The calculation proposed in this study safely predicts the slipping strengths of the connections of all specimens. Using Equation (1), a retrofitting designer can choose the failure modes of the yielding and buckling of knee braces, which act as energy absorbers.

**Figure 8.** Relationships between Q and Δ_H : (a) SL-45-1, SL-45-2, and SL-45-3; (b) SL-30.

The test parameter for observing the yield and buckling at the knee brace is the thickness, h , of the central part of the knee braces, 6, 9, 12, and 15 mm, corresponding to

the names of the specimens: nSL-6, nSL-9, nSL-12, and nSL-15. The loading program is illustrated in Figure 9. The test results are discussed by comparing them with the analytical results, which are numerically calculated in Section 3.

Table 4. Test results for slipping strength.

	Test Results (kN)	Slipping Strength (kN)	
		Average	Calculated Value
SL-45-1	59.9	56.3	46.6
SL-45-2	54.1		
SL-45-3	55.0		
SL-30	71.9	71.9	53.6

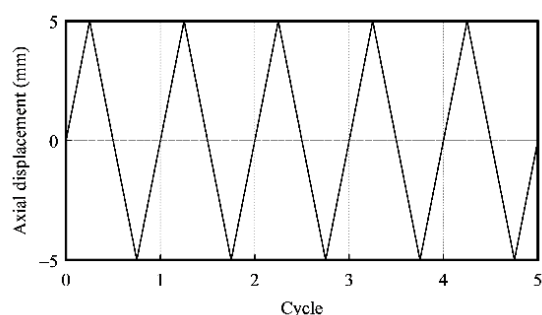


Figure 9. Loading program.

3. Analytical Study of Knee Brace and Discussion

An analytical study was conducted using the FEM program of Marc 2017.0.0., in which both material and geometric nonlinearities are considered. The main aim of the analytical investigation was to trace the load versus deformation relations of the knee braces obtained by the tests.

Figure 10 shows the analytical model of the knee brace. A solid element with ten nodes is used for the analytical model. An initial displacement, $L/1000$ (L is shown in Figure 7), is given in the orthogonal direction of the axis of the brace by considering that initial imperfections exist in the knee braces of the test specimens. The boundary conditions for the analysis are shown in Figure 11. The upper endplate is supported by rollers at four points, and the lower endplate is supported by pins at four points. The alternative displacements at the top of the knee brace are controlled to trace the load versus deformation relation of the test. The yield criterion follows von Mises stress, as shown in Figure 12.

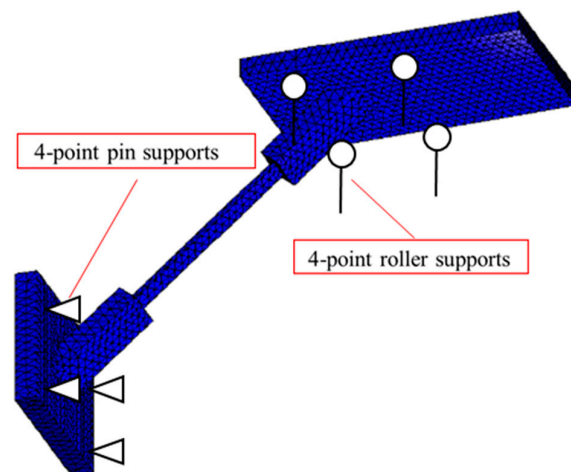


Figure 10. Element mesh and boundary conditions of analytical model.

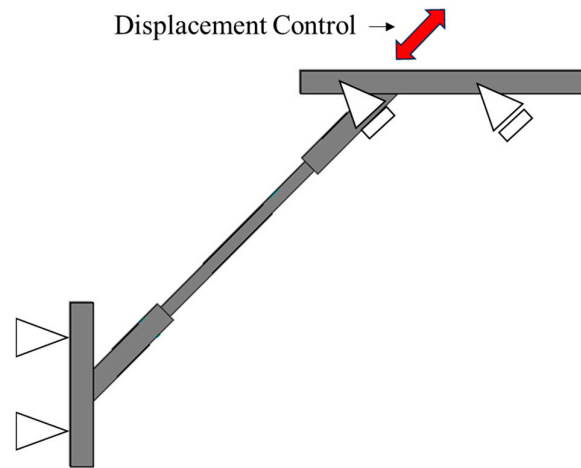


Figure 11. Boundary conditions and applied displacements of analytical study.

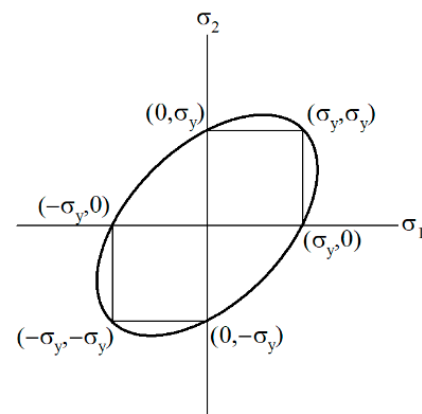


Figure 12. von Mises yield criterion.

Figure 13 shows the analytical results of the deformation and stress states using a contour diagram of the von Mises stress. The yellow and red areas indicate greater stress than the blue area. Figure 14 shows the buckling deformation during the test. The buckling deformations obtained from the test and the analysis show good agreement. Figure 15 shows the axial force, N , versus the axial displacement, Δ_A , relations of the knee braces for the experiments and analyses of nSL-6, 9, 12, and 15. The black and red lines in the figures represent the experimental and analytical results, respectively.

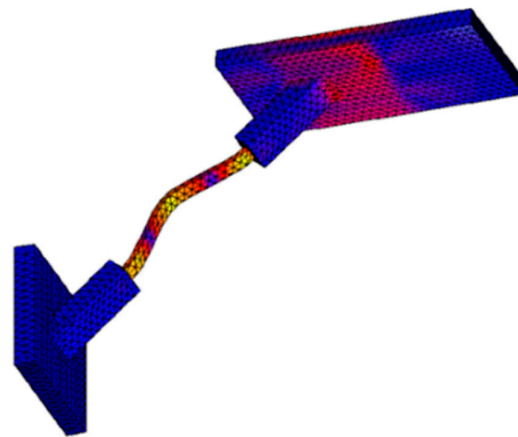


Figure 13. Deformation and stress contour analysis.



Figure 14. Buckling deformation test.

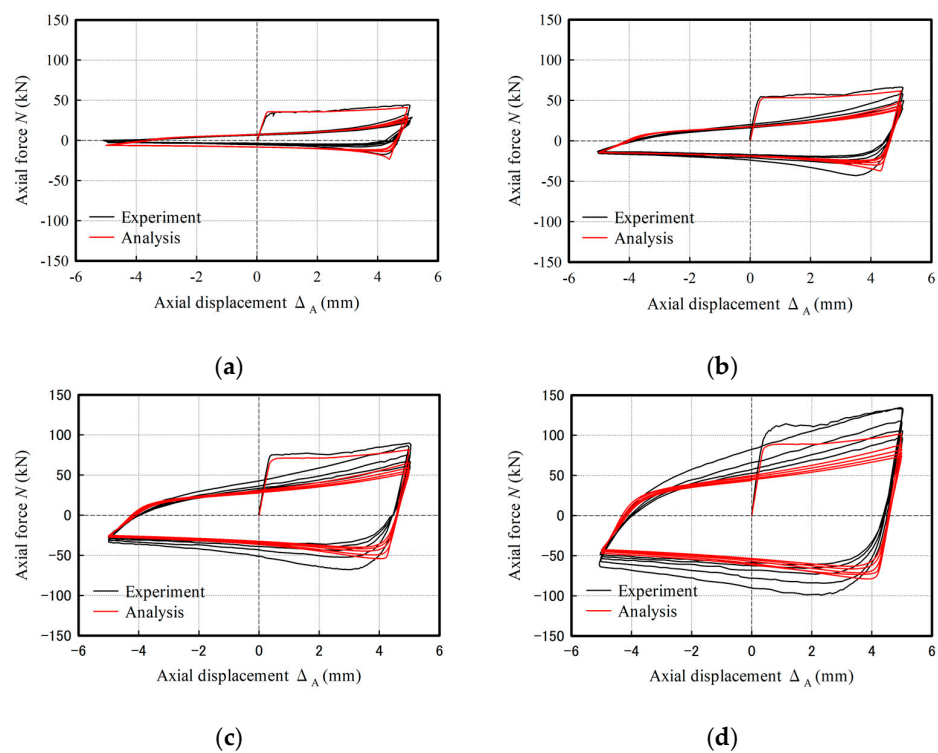


Figure 15. Relationships between N and Δ_A : (a) nSL6, (b) nSL-9, (c) nSL-12, and (d) nSL-15.

The values of N increase after yielding of the braces under tensile force owing to the strain-hardening effect. On the other hand, the values of N decrease after the buckling of the braces under compressive force. The tensile and buckling strengths of the four specimens increase with an increase in brace thickness. The analytical results match well with the experimental results.

The maximum values of the experimental and analytical results are summarized in Table 5. In the case of nSL-15, the test result is higher than the analytical result. This is because the test specimen was welded twice at the ends of the brace owing to the welding defects. The hardening effect caused by reheating is the reason why the test is stronger than the analysis. The yield strength of the test is over 6% of that of the analysis, except for that of nSL-15. The buckling strength of the analysis is smaller than that of the test results, except for nSL-6. This is because the initial displacement is assumed to be $L/1000$, which is too large for nSL-9 and nSL-12.

Table 5. Maximum values of experiment and analysis.

	Yield Strength (kN)			Buckling Strength (kN)		
	Exp.	Ana.	Exp./Ana. (%)	Exp.	Ana.	Exp./Ana. (%)
nSL-6	44.3	41.0	108	17.4	23.5	74
nSL-9	66.6	61.8	108	43.1	37.1	116
nSL-12	90.0	81.6	110	67.9	54.2	125
nSL-15	134	102	132	99.1	79.0	125

In our experimental and analytical results, the load versus deformation relationships show hysteretic loops that dissipate the input energy by their plastic behavior. The knee braces connected by the vises can exhibit effective energy absorption capacities, as shown in the results of recent studies [7–14].

After the tests, the buckled braces can be removed easily. The advantage of this method is not only the good attachment but also the detachment of the retrofitting members. Thus, this method can improve the resiliency of the building after large earthquakes due to its ability to replace the retrofitting devices.

4. Relaxation Test of Vise and Discussion

The long-term performance of joints that use bolts in steel structures has been widely studied through relaxation tests, including tests of high-strength bolts reported by Chesson [19] and Nah [20].

In Chesson's study [19], a stress relaxation test was conducted using high-strength A325 bolts. The short-term stress relaxation of these bolts introduced to a tension of 5000 pounds was examined. The experimental results showed that, after 1 min of tightening, the tensile stress in the bolts decreased by between 2% and 11%, with an average of approximately 5%. In Nah's study [20], relaxation tests were conducted on ASTM (American Society for Testing and Materials) A490 bolts [21]. The experimental parameter was the surface situation on tightened steel plates. The results showed that, after 1000 h, the retention rate was 86% for specimens without surface treatment and 81% for specimens with surface treatment.

Our proposal for joints applied using a vise is unique, as no previous study investigates the stress relaxation of the vise. Therefore, the long-term performance of the connection made using the vise was investigated through relaxation testing.

In the relaxation tests, two steel cuboids were prepared to measure the axial forces of the vise bolts. The dimensions of the cuboids were 44.8 mm and 44.4 mm in height, with cross sections of 27.6 × 26.9 mm and 27.5 × 26.4 mm, respectively. As shown in Figure 16, a steel plate with a thickness of 6 mm and the cuboid were clamped using the vise, and the axial force of the device was measured using strain gauges glued on four sides of the steel cuboid. Figure 17 shows the test setup, where the temperature was also measured using a thermocouple. The observations of strain and temperature were conducted over three months.

Figures 18 and 19 show the axial force versus the time relations of the two specimens. The vertical axis shows the axial force (kN), which was calculated by multiplying the average value of the four strain gauges by the axial stiffness of the cuboid. The horizontal axis shows the observation time. The initial axial forces were 75.2 kN and 77.7 kN for the two specimens, respectively. The average was 76.5 kN, close to the value of 75 kN, which is the nominal value of the initial force introduced by a torque of 300 Nm. The horizontal axis in Figure 18 shows the time (s) from 0 s to 300 s. The decreases in the axial forces of specimen 1 and specimen 2 were 2.6 kN and 1.7 kN, and the rates of decrease were 3.5% and 2.1%, respectively. No rapid drop in the axial force was observed for approximately five minutes after the introduction of the axial force. The decrease in the axial force was not as large as in the relaxation tests of high-strength bolt-joints reported by Chesson [19].



Figure 16. Photo of relaxation test.



Figure 17. Test setup of relaxation experiment.

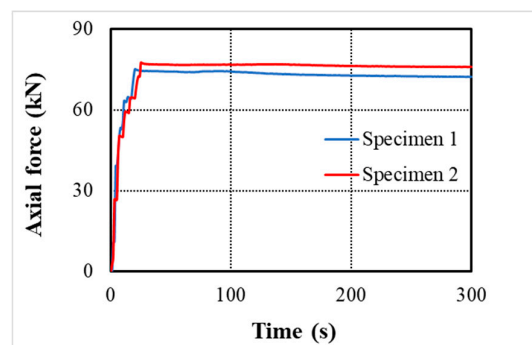


Figure 18. Axial force–time relationship over 300 s.

Figure 19 shows the axial force versus time (h) relationship recorded over three months, where the maximum value of the horizontal axis is 2200 h. The strain fluctuations of the test specimens have the same tendency as the temperature change observed by the thermocouple, and then the axial strain is corrected by considering a linear expansion coefficient of $10^{-5}/^{\circ}\text{C}$. The retention rates of the two specimens were 92% and 94%, respectively. The stress relaxation tests showed the long-term connecting performance of the vise, in which the clamping force was maintained at over 90% of the initial force over three months. This result shows the same level of performance as the stress relaxation test of joints with high-strength bolts described by Nah [20].

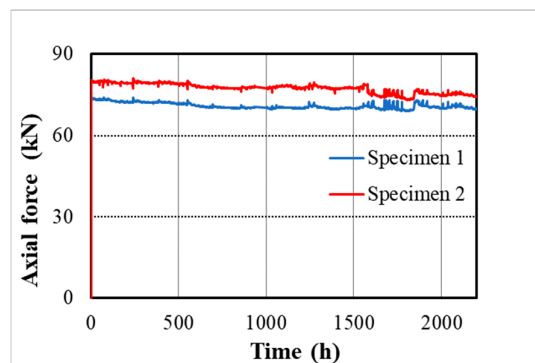


Figure 19. Axial force–time relationship over 2200 h.

5. Conclusions

In this study, a novel approach is proposed involving the use of knee braces attached to high-hardness vises. This is only applicable to open-frame steel structures. A feature of the retrofitting method is its easy setup owing to the use of vises. The boltheads of the vises, which are made from high-hardness metal, grip tightly between the steel plates of the connections. Testing and analysis were conducted to investigate the structural properties of the proposed method. Two failure modes were experimentally observed through the testing of specimens retrofitted using the knee braces: the slipping behavior at the connection and the yielding and buckling behavior at the knee brace.

The slipping strength between the endplate of the knee brace and the existing steel beam was investigated, and the slipping strengths at different angles were safely estimated using the calculating method proposed in our previous paper.

Nonlinear FEM analysis was conducted to evaluate the energy absorption performance of the knee braces. The characteristics of the load versus deformation relationship obtained through the testing of the retrofitted frames matched well with the FEM analysis results. The strengths of the yielding and buckling of the knee braces and the energy dissipating capacities of this retrofit were estimated using the FEM analysis. The knee braces connected by the vises showed the same level of energy dissipating capacity as those reported in previous studies.

Additionally, long-term relaxation tests were performed to investigate the practical use of the proposed method. The vises maintained their clipping forces at over 90% of the initial forces in the stress relaxation tests over 2200 h. No rapid loss in the clipping force of the vises was observed during the first five minutes of the relaxation test. The long-term performance of the vises was the same as that of high-strength bolts reported in previous studies.

The new seismic retrofitting method using vises made from high-hardness metal provides an easy construction technique with efficient seismic performance.

Author Contributions: H.N. designed the study. H.N., D.N. and I.C. were involved in analytical work, calculations, and data interpretation. All authors critically revised the manuscript, commented on the drafts of the manuscript, and approved the final paper. All authors have read and agreed to the published version of the manuscript.

Funding: This research received no external funding.

Data Availability Statement: The data that support the findings of this study are available from the corresponding author upon reasonable request.

Acknowledgments: The authors wish to express their gratitude to Touki Kawano, a student at Nagasaki University, and Kenta Okamoto, a technician at Nagasaki University, for their contributions to the experimental study.

Conflicts of Interest: The authors declare no conflicts of interest.

Appendix A

To ensure the seismic performance of steel structures joined using vises, it is important to confirm that the vises are not damaged from practical use. The mechanical performance of the vises was investigated using FEM analysis in Marc software. The dimensions of the vise are shown in Figure A1, and Tables A1–A3 summarize the chemical composition and mechanical properties of the vise.

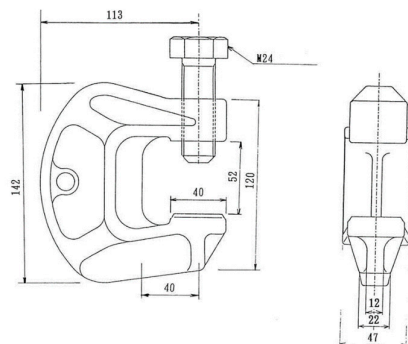


Figure A1. Dimensions of vise with high-hardness screw bolt.

Table A1. Chemical composition of vise (%).

	C	Si	Mn	P	S	Cu	Ni	Cr	Mo
Standard (%)	0.37~ 0.44	0.15~ 0.35	0.55~ 0.95	≤0.03	≤0.03	≤0.30	≤0.25	0.85~ 1.25	0.15~ 0.35
Measured (%)	0.41	0.26	0.7	0.019	0.015	0.11	0.08	1.11	0.17

Table A2. Chemical composition of bolt (%).

	C	Si	Mn	P	S	Cu	Ni	Cr	Mo
Standard (%)	0.37~ 0.44	0.15~ 0.35	0.55~ 0.95	≤0.03	≤0.03	≤0.30	≤0.25	0.85~ 1.25	0.15~ 0.35
Measured (%)	0.42	0.29	0.8	0.023	0.014	0.1	0.06	1.01	0.18

Table A3. Mechanical properties (JIS standard: reference value).

Spec	Tensile Test (No. 4 Test Piece)				Hardness Test
	σ_y (N/mm ²)	σ_u (N/mm ²)	Elongation (%)	Contraction (%)	Hardness (HB)
SCM440	834	980.7	12 more	45 more	285~352

There are two different loadings of the analysis, as shown in Figure A2. A force corresponding to shearing deformation, shown in Figure A2 (a), is applied if slipping occurs between the two steel plates. A force corresponding to tensile deformation, shown in Figure A2 (b), is applied when the axial force of the bolt is introduced by a torque wrench. Under these loading conditions, the stress state and load versus deformation relationships are discussed through numerical analysis.

The main body of the vise is analyzed by a mesh model with 10 nodes of solid elements, as shown in Figure A3. As shown in Figure A4, analytical supports are set at the top and bottom of the open part of the C shape of the vise. The four points at the bottom of the open part are fixed by pin supports. A horizontal sliding support is applied in the analysis of (a), and a vertical sliding support is applied in the analysis of (b). When the displacements are applied at the top of the vise, the reaction and relative displacements are obtained in each

direction. The von Mises yield condition is used. The stress–strain model is defined as a bilinear elastoplastic model in Figure A5, and the material properties are listed in Table A4. The strain-hardening coefficient is the inclination of the line between the yielding point and the tensile strength corresponding to a strain of 20%. The relationship between true stress and logarithmic strain is applied to the analysis.

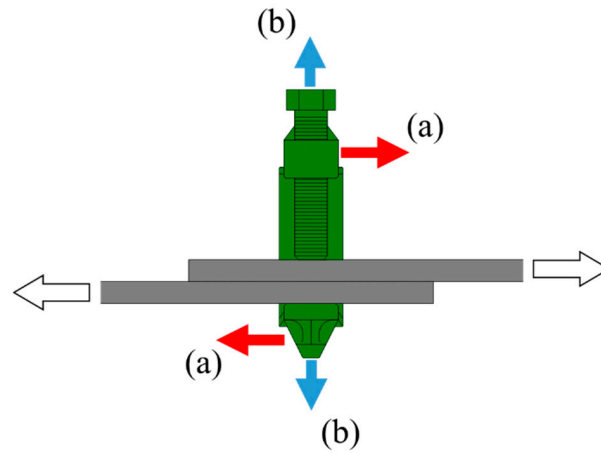


Figure A2. Applied forces to vise: (a) slipping force; (b) axial force.

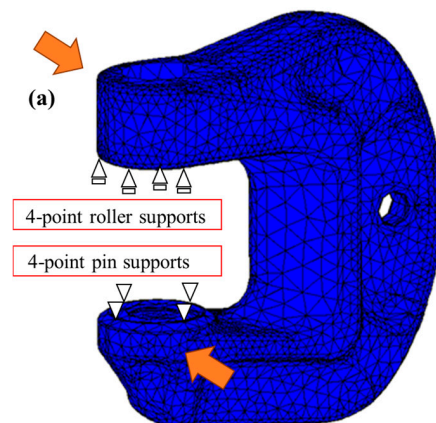


Figure A3. Boundary condition and direction of applied force in FEM mesh model of vise.

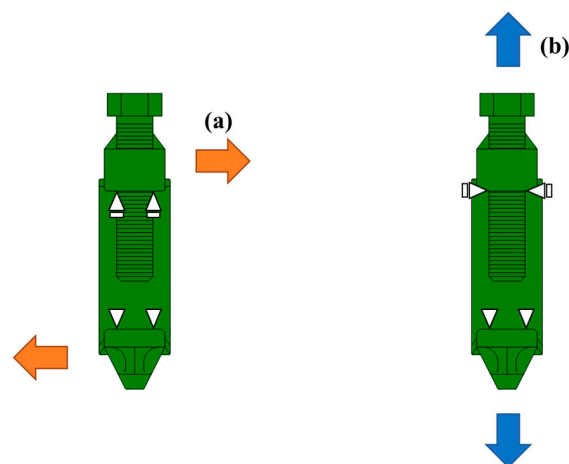


Figure A4. Boundary condition and direction of force in vises: (a) slipping force; (b) axial force.

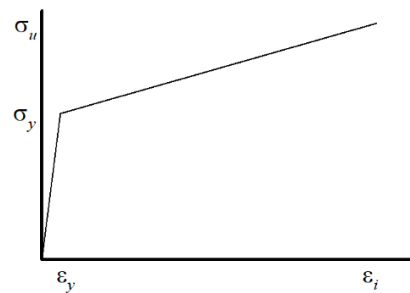


Figure A5. Bilinear stress–strain model.

Table A4. Constants in the material model.

σ_y (N/mm ²)	σ_u (N/mm ²)	ϵ_t (%)
834	980.7	20

σ_y : yield strength; σ_u : tensile strength; ϵ_t : strain at the tensile stress.

Figure A6 presents the load–displacement relationship in the direction of (a). In the figure, softening behavior is observed at approximately 30 kN; however, after that, the strength increases almost linearly up to 80 kN. After the steel plates joined by the vises start to slip, the bolt sustains a horizontal force. In this case, the main body of the vise, which provides twisting deformation, is subjected to the shearing force shown in Figure A2 (a) and Figure A4 (a).

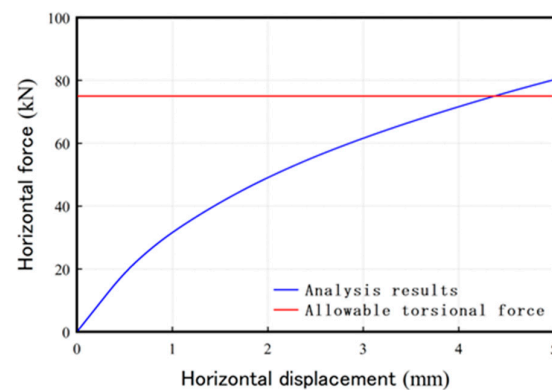


Figure A6. Load–displacement relationship under force applied in direction of (a).

In the study of the vise itself, an allowable force of shear is set as 75 kN per vise. The force of the screw bolt of the vise in the direction orthogonal to the bolt was defined as the “digging strength”, which was described in a study conducted by Uno [22]. The digging strength corresponds to the axial force of the bolts of 75 kN, since the shape of the bolthead is triangular at 45-90-45.

As shown in Figure A6, even when the shearing force reaches 75 kN, the vise maintains its strength. Figure A7 presents a contour diagram of von Mises stress at a displacement of 4 mm in case (a). In the figure, some parts of the vise are yielding; however, the stresses in most parts remain elastic. This indicates that no practical problems arise when using a vise for seismic retrofitting.

Figure A8 shows the load–displacement relationship in the direction of (b). The opening deformation of the vice is caused by a reaction from the axial force of the screw bolts introduced from a torque wrench. In the figure, the opening force remains elastic up to 200 kN. Thus, an allowable axial force of the bolt is set as 200 kN. This is shown by the solid red line in Figure A8. Since the compressive force introduced into the bolt is 75 kN (red dotted line in Figure A8) during normal use of the vise, there is a sufficient margin in terms of strength.

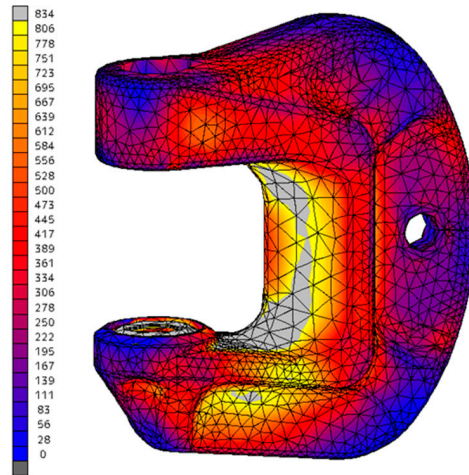


Figure A7. Contour diagram of von Mises stress at a displacement of 4 mm in case of (a).

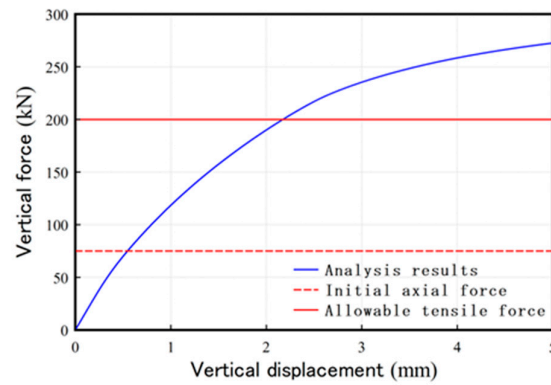


Figure A8. Load–displacement relationship under force applied in direction of (b).

Figure A9 shows a contour diagram of the von Mises stress at a displacement of 2 mm in case (b). In this figure, the yielding parts are displayed along the inside of the vise; however, the stresses of the other parts remain under yielding stress at a load of 200 kN. The applied load is 75 kN under normal use. Even if a double load is applied, the vise retains its connecting performance.

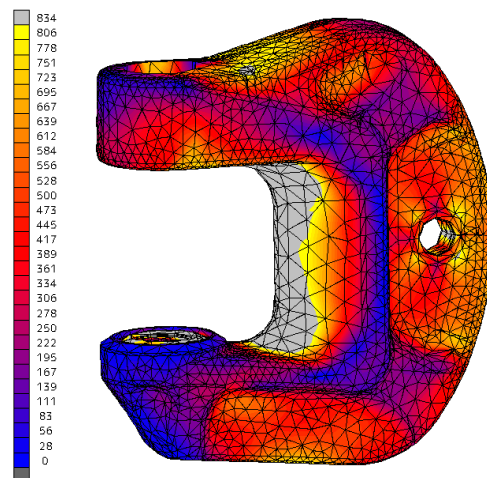


Figure A9. Contour diagram of von Mises stress at a displacement of 2 mm in the case of (b).

References

1. Steel Committee of Kinki Branch the Architectural Institute of Japan (AIJ). *Reconnaissance Report on Damage to Steel Building Structures Observed from the 1995 Hyogoken-Nanbu (Hanshin/Awaji) Earthquake*; Steel Committee of Kinki Branch the Architectural Institute of Japan (AIJ): Kyoto, Japan, 1995.
2. Fang, C.; Wang, W.; Qiu, C.; Hu, S.; MacRea, G.A.; Eatherton, M.R. Seismic resilient steel structures: A review of research, practice, challenges and opportunities. *J. Constr. Steel Res.* **2022**, *191*, 107172. [[CrossRef](#)]
3. MacRae, G. Low Damage Design of Steel Structures. Steel Innovations 2013 Workshop, Christchurch, New Zealand. Available online: https://www.scnz.org/wp-content/uploads/2020/11/Low-Damage-Design-of-Steel-Structures_MacRae_Clifton.pdf (accessed on 3 July 2024).
4. Domenico, D.; Ricciardi, G.; Takewaki, I. Design strategies of viscous dampers for seismic protection of building structures: A review. *Soil Dyn. Earthq. Eng.* **2019**, *118*, 144–165. [[CrossRef](#)]
5. Kishiki, S.; Uehara, D.; Yamada, S.; Suzuki, K.; Saeki, E.; Wada, A. Behavior of beam splices with energy dissipating elements at the bottom flange. *J. Struct. Constr. Eng. AIJ* **2005**, *70*, 135–143. [[CrossRef](#)] [[PubMed](#)]
6. Tamai, H.; Takamatsu, T.; Murata, M.; Kadoya, H. On Hysteretic dampers for steel buildings with bent steel plates (Part1 Loading tests on bent steel plate). *Bull. Hiroshima Inst. Technol.* **2010**, *44*, 151–156.
7. Shin, J.; Lee, K.; Jeong, S.H.; Lee, H.S.; Kim, J.K. Experimental and analytical studies on buckling-restrained knee bracing systems with channel sections. *Int. J. Steel Struct.* **2012**, *12*, 93–106. [[CrossRef](#)]
8. Hsu, H.; Juang, J.; Chou, C. Experimental evaluation on the seismic performance of steel knee braced frame structures with energy dissipation mechanism. *Steel Compos. Struct.* **2011**, *11*, 77–91. [[CrossRef](#)]
9. Zhang, L.; Tong, G.S. Out-of-plane stability of simply supported beams with knee braces. *J. Constr. Steel Res.* **2007**, *63*, 175–181. [[CrossRef](#)]
10. Clement, D.E.; Williams, M.S. Seismic design and analysis of a knee braced frame building. *J. Earthq. Eng.* **2004**, *8*, 523–543. [[CrossRef](#)]
11. Kim, J.K.; Seo, Y.G. Seismic design of steel structures with buckling-restrained knee braces. *J. Constr. Steel Res.* **2003**, *59*, 1477–1497. [[CrossRef](#)]
12. Hsu, H.-L.; Li, Z.-C. Seismic performance of steel frames with controlled buckling mechanisms in knee braces. *J. Constr. Steel Res.* **2015**, *107*, 50–60. [[CrossRef](#)]
13. Honma, S.; Ebato, K.; Harada, Y. Ductile steel knee brace with built-in comb-shaped seismic damper. *J. Constr. Steel Res.* **2021**, *184*, 106765. [[CrossRef](#)]
14. Li, R.; Yuan, Z.; Qi, L.; Yuan, C.; Xue, J. Improvement effects of knee-bracing friction dampers on cyclic behavior of steel joints in antique buildings. *Structures* **2024**, *60*, 105919. [[CrossRef](#)]
15. Harada, Y.; Ebato, K.; Honma, S.; Takimoto, T. Experimental Study on Seismic Retrofit by Using Supplemental Knee Braces Attached to Steel Members with Semi-Rigid Bolted Connections. In Proceedings of the 15th World Conference on Earthquake Engineering, Lisbon, Portugal, 24–28 September 2012; Volume 5.
16. Yamada, S.; Shimizu, K.; Takei, Y. Seismic Retrofitting Effect of Reinforcing Over-Track Buildings with Knee-Brace Dampers. *Q. Rep. RTRI* **2011**, *52*, 217–223. [[CrossRef](#)]
17. Nakahara, H.; Ding, N.; Shimomura, T. Seismic retrofitting method for steel structures by knee braces jointed by high hardness vises. *J. Civ. Eng. Manag.* **2022**, *29*, 67–76. [[CrossRef](#)]
18. AISC-Research Council on Structural Connections. *Load and Resistance Factor Design Specification for Structural Joints Using ASTM A325 or A490 Bolts*; AISC-Research Council on Structural Connections: Chicago, IL, USA, 1994.
19. Chesson, E.; Munse, W.H. Studies of the behaviour of high strength bolts and bolted joints. In *Engineering Experiment Station Bulletin 469*; University of Illinois College of Engineering: Chicago, IL, USA, 1964.
20. Nah, H.S.; Lee, H.J.; Kim, K.S. Evaluation of Long-term Relaxation for High-strength Bolted Connections. In Proceedings of the ICAPP '10, San Diego, CA, USA, 13–17 June 2010.
21. AISC-Research Council on Structural Connections. *Specification for Structural Joints Using ASTM A325 or A490 Bolts*; AISC-Research Council on Structural Connections: Chicago, IL, USA, 2004.
22. Uno, N.; Inoue, K.; Shimura, Y.; Wakiyama, K. Coefficient of friction between steels with different hardness. *J. Struct. Constr. Eng. AIJ* **1997**, *494*, 123–128. [[CrossRef](#)] [[PubMed](#)]

Disclaimer/Publisher's Note: The statements, opinions and data contained in all publications are solely those of the individual author(s) and contributor(s) and not of MDPI and/or the editor(s). MDPI and/or the editor(s) disclaim responsibility for any injury to people or property resulting from any ideas, methods, instructions or products referred to in the content.